Chapter 2

Infrared High-Index Coating Materials, PbTe and $Pb_{1-x}Ge_xTe$: Properties and Applications

Bin Li, Ping Xie, Suying Zhang and Dingquan Liu

Additional information is available at the end of the chapter

http://dx.doi.org/10.5772/intechopen.79272

Abstract

The greater value of refractive index for high-index layers in thin-film interference filters operating in the infrared has an incomparable advantage. Lead telluride (PbTe), which is much superior to other infrared high-index coating materials due to its high index and advantage of fundamental absorption edges, has played an important role in filters employed in the infrared radiometer and other instruments launched in space atmosphere sounding research projects. In this chapter, we summarized some recent achievements in the investigations into another infrared high-index coating material—lead germanium telluride ($Pb_{1-x}Ge_xTe$), a pseudo-binary alloy of PbTe and GeTe. It can be revealed that the layers of $Pb_{1-x}Ge_xTe$ exhibit the tunable optical properties, such as temperature coefficient of refractive index and fundamental absorption edge, as well as mechanical properties, such as the hardness and Young's modulus, corresponding to its intrinsic ferroelectric phase transition. Some important applications in thin-film interference filters were also demonstrated for its tremendous potential, such as a stable narrow bandpass interference filter without temperature-induced wavelength shift and a tunable infrared short wavelength cutoff filter. Furthermore, it is also revealed that electron beam evaporation is a more effective congruent-transfer technique to deposit the layers of $Pb_{1-x}Ge_xTe$.

Keywords: infrared, thin-film interference filter, lead-telluride, lead-germanium-telluride

1. Introduction

The rapid detection of the dynamites or explosives is of increasing importance in the anti-terror campaign. A technology to detect the trace dynamites can be developed using the electromagnetic radiation in the mid-wavelength infrared region, because many strong fundamental absorption bands with regard to "fingerprint" are included in this range [1]. Although,

in recent years, a significant progress has been achieved toward the miniaturization of infrared spectrometers, which can play an important role in the homeland security and law enforcement, accompanied with the development of thermoelectrically cooled detectors and quantum cascade lasers, a thin-film narrow bandpass interference filter, which has a passband coinciding with and as narrow as the typical absorption line of "fingerprint," is urgently needed to increase sensitivities of the spectrometers. An order of magnitude larger angular dispersion than gratings can be carried out due to the characteristic lines assigned to the trace dynamites being distinguished using a thin-film bandpass filter. Therefore, the spectral fluctuation will be reduced considerably and a greater level of miniaturization can be completely obtained without the clumsy gratings [2]. Furthermore, more profits can also be gained out of thin-film filters, because of their cost-efficient mass-production compared with the gratings.

According to Macleod [3], the simplest type one-cavity all-dielectric Fabry-Perot filter has the form of $[HL]^N 2mH[LH]^N$ or $H[LH]^N 2mL[HL]^N H$, where H and L being quarter-wavelength layers with high and low refractive indices, respectively, m is the order of the spacer, and N is the number of full periods in the reflecting stacks. Therefore, the expressions for the halfwidth of a Fabry-Perot filter can be presented as Eq. (1) for high refractive index spacer,

$$\left(\frac{2\Delta\lambda}{\lambda_0}\right)_{\mathrm{H}} = \frac{4\mathrm{n_s}}{m\pi(\mathrm{n_H}/\mathrm{n_L})^{2\mathrm{N}}\mathrm{n_H}}\left(\frac{(\mathrm{n_H}/\mathrm{n_L})-1}{(\mathrm{n_H}/\mathrm{n_L})-\frac{\mathrm{m}-1}{\mathrm{m}}}\right) \tag{1}$$

and Eq. (2) for low-refractive-index spacer,

$$\left(\frac{2\Delta\lambda}{\lambda_0}\right)_{\mathrm{L}} = \frac{4\mathrm{n_s}}{m\pi(\mathrm{n_H}/\mathrm{n_L})^{2\mathrm{N}}\mathrm{n_L}}\left(\frac{(\mathrm{n_H}/\mathrm{n_L})-1}{(\mathrm{n_H}/\mathrm{n_L})-\frac{\mathrm{m}-1}{\mathrm{m}}}\right) \tag{2}$$

where λ_0 being the central wavelength, and n_H and n_L being the indices of refraction of the high-index layers, low-index layers in the filter, and respectively, and n_s, that of the substrate. Therefore, in order to reduce the halfwidth of a Fabry-Perot filter, it is almost always advantageous for its high-index layers to use a coating material with the highest value of refractive index available in the spectral regions of interest. That is, the greater the value of n_H/n_L is, the narrower the halfwidth can be obtained.

Although, conveniently, germanium (Ge) is a preferred choice of coating material for the high-index layers in the spectral region of mid-wavelength infrared due to its higher value (round 4.0) of refractive index, it is still expected that another material with an even higher index is available to substitute for Ge in order to further reduce the halfwidth of a filter.

2. Properties and applications of PbTe

Lead telluride (PbTe) is one of lead chalcogenides, which has been widely investigated as a conventional semiconducting material for many decades. The mineralogical name of PbTe is Altaite, a yellowish white mineral with an isometric crystal structure, which was discovered in 1845 in the Altai Mountains [4].

PbTe is a promising material candidate for mid-wave infrared detection because of their superior chemical and mechanical stability over HgCdTe alloys [5–7]. In addition, as a simple *p*-type thermoelectric material with the large Grüneisen parameter and high valley degeneracy, PbTe has demonstrated exceptional thermoelectric performance with an optimized peak zT of ~1.4 [8–10].

However, PbTe is also one of high-index infrared coating materials. Currently, it dominates the material selection for the design of infrared thin-film interference filters operating in the long wavelength infrared both at room and reduced temperature. The combination of its high index (above 5.5 in the spectral range of long wavelength infrared at room temperature) and its advantage of a negative temperature coefficient of refractive index (-2.0×10^{-3} K^{-1}) make it much superior to other infrared coating materials [11–17].

In **Figure 1(a)**, it can be illustrated that a layer of PbTe has a very high value of refractive index [13], although it is lower than that of bulk single crystal of PbTe [18]. In **Figure 1(b)**, it can be also revealed that the foundational absorption edge of the layer of PbTe will shift toward the longer wavelength with the decreasing ambient temperature. Therefore, a single layer of PbTe can be regarded as a natural selective absorption longwave-pass cutoff filter to omit the auxiliary filters which are necessary to block the unfavorable Planck emission from hot resources.

Since the middle of the twentieth century, using PbTe as the infrared high-index coating materials, Infrared Multilayer Laboratory at the University of Reading, Reading, United Kingdom, have completed spectral design and manufacture of high-quality infrared thin-film interference filters for complex infrared radiometer and ground-based astronomical instruments in over 30 major UK and international space and astronomical research projects [19]. In **Figure 2**, the space and astronomical research projects being launched in the recent 5 years, in which infrared thin-film interference filters were manufactured in Infrared Multilayer Laboratory using PbTe as the infrared high-index coating materials, were listed.

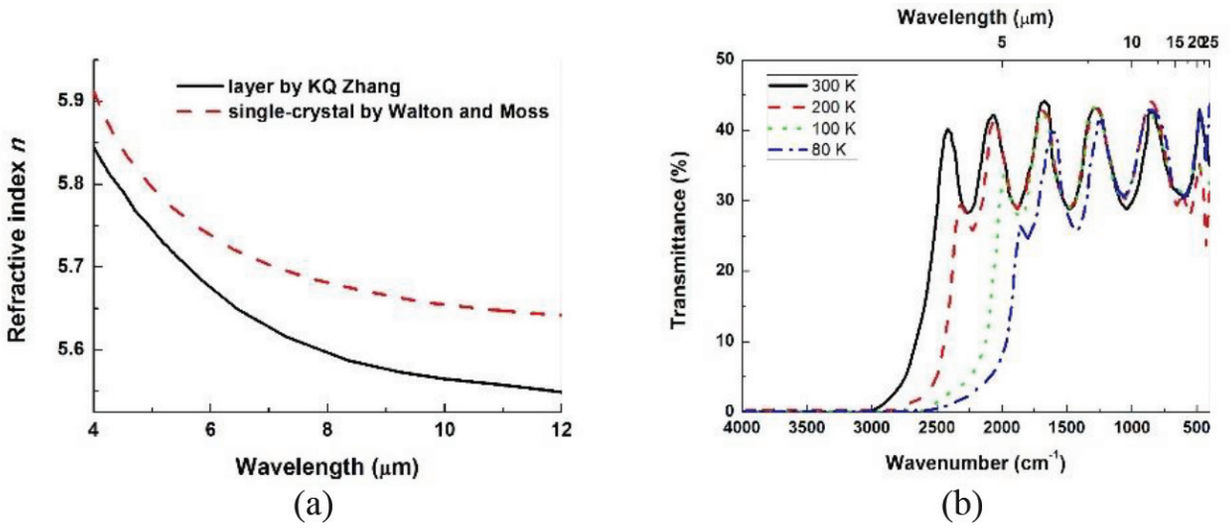

Figure 1. (a) A comparison of refractive index of a single layer of PbTe with that of bulk single crystal; (b) the shift of foundational absorption edge of a layer of PbTe with the decreasing ambient temperature.

Figure 2. The space and astronomical research projects in the recent 5 years, in which infrared thin-film interference filters were manufactured in infrared multilayer laboratory using PbTe as the infrared high-index coating materials.

However, if the conventional PbTe materials are used as the evaporants, which are prepared from the stoichiometric proportions of pure constituents, a strong *n*-type Pb-rich layer will be deposited even at a very low substrate temperature, for example, 100°C. Because an excess of nonstoichiometric carrier absorption emerges, these Pb-rich layers are completely opaque beyond 12 μm. Therefore, in order to obtain good-quality PbTe layers, a compensative process is required, which is commonly carried out either by introducing oxygen into the evaporation chamber in the course of the deposition of a PbTe layer or by baking the layers in air after deposition has been finished. However, the practice of postdeposition annealing is not ideal when the requirements for precise and reproducible spectral positioning and shape of a required filter profile are tightly specified and the introduction of oxygen raises a complexity in the technological process. In addition, both oxidizing processes cause the presence of lead oxide on the surface of the layer [20].

Since the partial pressures of Pb and Te_2 strongly depend on the properties of the evaporants, it is possible to shift the characteristics of the deposited layers by using a PbTe material with a Te dopant. Therefore, a kind of evaporable PbTe material with "mild" characteristics has been developed in Shanghai Institute of Technical Physics, Chinese Academy of Sciences, Shanghai, China [21, 22]. By "mild," we mean that, in a rather broad region of substrate-temperature, the

Figure 3. Some products of evaporation materials of "mild" PbTe.

concentration of free carriers in the layers from such a material can be 25–40 times lower than in normal PbTe materials. In **Figure 3**, some products of "mild" PbTe evaporation materials were exhibited.

3. Properties and applications of $Pb_{1-x}Ge_xTe$

Lead germanium telluride ($Pb_{1-x}Ge_xTe$) is a pseudo-binary alloy of IV-VI narrow-gap semiconductor compounds, PbTe and GeTe [23].

Like some IV–VI compound semiconductors, for example, the tellurides of Sn and Ge and their alloys, $Pb_{1-x}Ge_xTe$ shows also a ferroelectric phase transition from a high-temperature cubic, rock salt (O_h) structure above a Curie temperature T_C to a low-temperature rhombohedral, arsenic-like (C_{3v}) phase. The rhombohedral structure originates from a displacement of two sublattices along a <111> direction that becomes the *c* axis. In particular, for $Pb_{1-x}Ge_xTe$, the Curie temperature T_C increases steeply with increasing Ge concentration. The phase transition is driven by off-center site occupation of Pb ion sites by Ge ions. Anomalies happen in the electrical resistivity and specific heat of $Pb_{1-x}Ge_xTe$ alloys corresponding to the ferroelectric phase transition [24–32].

In this chapter, some investigations into the optical and mechanical properties of the layers of $Pb_{1-x}Ge_xTe$, which have been carried out in Shanghai Institute of Technical Physics, Chinese Academy of Sciences, Shanghai, China, were demonstrated; furthermore, some applications of $Pb_{1-x}Ge_xTe$ as the infrared high-index coating materials were also exhibited.

3.1. Low-temperature dependence of mid-infrared optical constants of layers of $Pb_{1-x}Ge_xTe$

Although many investigations, both theoretical and experimental, have been carried out on the mechanism of ferroelectric phase transition of $Pb_{1-x}Ge_xTe$, the investigation into the optical constants (refractive index *n* and absorption coefficient *k*) of the layers of $Pb_{1-x}Ge_xTe$ as a function of temperature remains to be done [33].

In our investigation, a layer of $Pb_{1-x}Ge_xTe$ was deposited on a silicon wafer using molybdenum boat heating the ingot of $Pb_{1-x}Ge_xTe$ ($x = 0.12$), of which composition was analyzed using proton-induced X-ray emission (PIXE) at the NEC 9SDH-2 pelletron tandem accelerator and can be represented with $Pb_{0.94}Ge_{0.06}Te$. The optical transmission spectra of the layer were measured using a Fourier-transform infrared spectrometer (BIO-RAD, FTS-40) in the range of 4000–400 cm^{-1} at normal incidence between 80 and 300 K accompanied by using a bath cryostat (Oxford, DN1704). The optical constants of the layer were determined through the fitting of transmission spectra recorded at different temperature using the Lorentz-oscillator model as the dispersion model for the complex frequency dependent dielectric functions.

As a consequence, the temperature dependence of optical constants can be obtained at low-temperature in the spectral range of 2.5–8.5 μm. It can be found that the layer of $Pb_{1-x}Ge_xTe$ has a refractive index with a value of 5.350–6.000 corresponding to different measured

temperatures in the spectral range of 4.0–8.5 μm, in which dispersion originated from the Reststrahlen and the absorption edge can be negligible. At room temperature, the layers of $Pb_{1-x}Ge_xTe$ have a value of refractive index approaching to that of layers of PbTe. A conclusion can be drawn that $Pb_{1-x}Ge_xTe$ is also an infrared high-index coating material.

In **Figure 4(a)**, the change of refractive index of the layers of $Pb_{0.94}Ge_{0.06}Te$ as a function of both wavelength and temperature was shown. It can be seen that the maximum value of refractive index occurs at 150 K, which can be regarded as the results of increased lattice polarizability that is an indication of the ferroelectric nature of the phase transition. Therefore, a conclusion can be drawn that anomalies in the refractive index, similar to those in the electrical resistivity and specific heat, emerge at the Curie temperature T_C of the layers of $Pb_{0.94}Ge_{0.06}Te$. In **Figure 4(b)**, the temperature coefficient of the refractive index, *dn/dT*, of the layers of $Pb_{0.94}Ge_{0.06}Te$ is given, from which one can find that the value of *dn/dT* is 20.006–0.002 K^{-1} in the spectral range of 3.0–8.5 μm at all measured temperatures.

An empirical formula for the temperature coefficient of refractive index in the spectral range of 4.0–8.5 μm can be expressed as Eq. (3):

$$\frac{dn}{dT} = f(\lambda, T) = A(T) + B(T)\lambda^{-C(T)} \tag{3}$$

where

$$A(T) = -0.05964 + 0.00156T - 1.41679 \times 10^{-5}T^2 + 5.24258 \times 10^{-8}T^3 - 6.76599 \times 10^{-11}T^4;$$
$$B(T) = 247.15385 - 6.75508T + 0.07137T^2 - 3.69672 \times 10^{-4}T^3 + 9.40269 \times 10^{-7}T^4 - 9.37957 \times 10^{-10}T^5;$$
$$C(T) = 156.18266 - 4.49072T + 0.05023T^2 - 2.65423 \times 10^{-4}T^3 + 6.6734 \times 10^{-7}T^4 - 6.44758 \times 10^{-10}T^5.$$

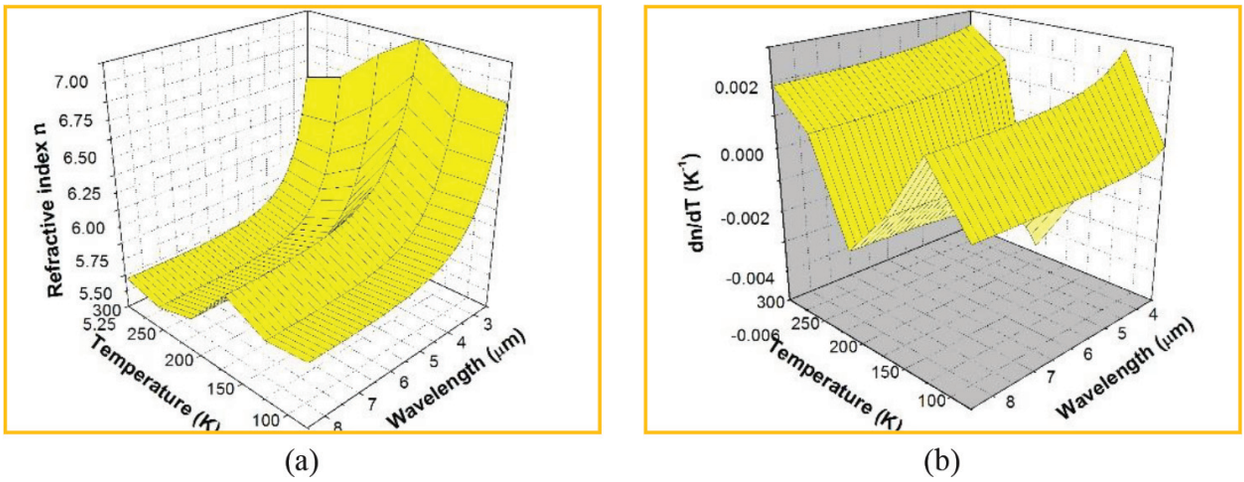

(a) (b)

Figure 4. (a) The change of refractive index of the layers of $Pb_{0.94}Ge_{0.06}Te$ as a function of both wavelength and temperature and (b) the temperature coefficient of the refractive index, *dn/dT*, of the layers of $Pb_{0.94}Ge_{0.06}Te$ (ref. [33], reuse permission obtained from AIP).

3.2. The stable narrow bandpass interference filters without temperature induced wavelength shift

When the ambient temperature varies, the performance of an optical thin-film interference filter will be also changed, such as the shift of center wavelength and the deterioration of peak transmission [34–36]. In particular, when a long wavelength infrared narrow bandpass filter is used in the spaceborne remote sensing instruments, the change of its spectral characteristics, which will lead to the difficulty to sustain the precision radiometric measurements from space, is not acceptable [37]. Addition of an auxiliary temperature control to the filters is not practical in order to maintain its stable optical performance in spaceborne remote sensing systems.

There are two factors that cause the shift of wavelength accompanied by the change of ambient temperature. One is the temperature-induced variations in the indices of refraction of the layers, and another is the variations in the physical thicknesses of the layers. Since the bulk temperature coefficients of linear expansion are an order of magnitude smaller than the temperature coefficients of the indices of refraction for substances similar to those usually employed for thin-film interference filters, it may be speculated that the shift of wavelength should be ascribed to the variations of temperature coefficients of the indices of refraction of the layers [38].

As far as the infrared filters employed in the spaceborne remote sensing systems are concerned, the convenient materials used for the low-index layers are either ZnS (2.2) or ZnSe (2.3). Moreover, Seeley et al. [39] modeled the sensitivity of the narrow bandpass filter to the change of temperature, showing that the spacer and the next two adjacent layers are dominant contributors relative to the other layers (and stacks). Therefore, when a negative shift in PbTe resulting from the negative temperature coefficient of refractive index is suitably combined with a positive shift in ZnS (or ZnSe) from its positive coefficient, temperature-invariant compensation becomes possible; namely, to achieve a negligible wavelength shift with temperature.

However, as a matter of fact, the temperature coefficient of refractive index of PbTe cannot exactly compensate for that of ZnS (ZnSe). Therefore, another solution to the problem is to seek a coating material of which the temperature coefficient of refractive index can be tuned.

Since the maximum value of refractive index of layers of $Pb_{1-x}Ge_xTe$ occurs corresponding to the structural phase transition, as a consequence, at the designated low-temperature, the temperature coefficient of refractive index of layers of $Pb_{1-x}Ge_xTe$ can be tuned from negative to positive by varying the Ge composition, that is, the layers of $Pb_{1-x}Ge_xTe$ with the specific composition may be used as the high-index layers in the thin-film interference filters.

Since the component elements in a multicomponent alloy system will evaporate at a different rate, which causes changes in compositions of layers relative to the evaporants, and it is in great necessity to designate directly the compositions in evaporated layers of $Pb_{1-x}Ge_xTe$. For example, the corresponding stoichiometry of evaporated layers can be expressed by the formula $(Pb_{1-x}Ge_x)_{1-y}Te_y$.

In **Figure 5**, the spectral characteristics of a simple one-cavity Fabry-Perot filter on a Ge substrate was demonstrated in the temperature range of 85–300 K, which was designed with

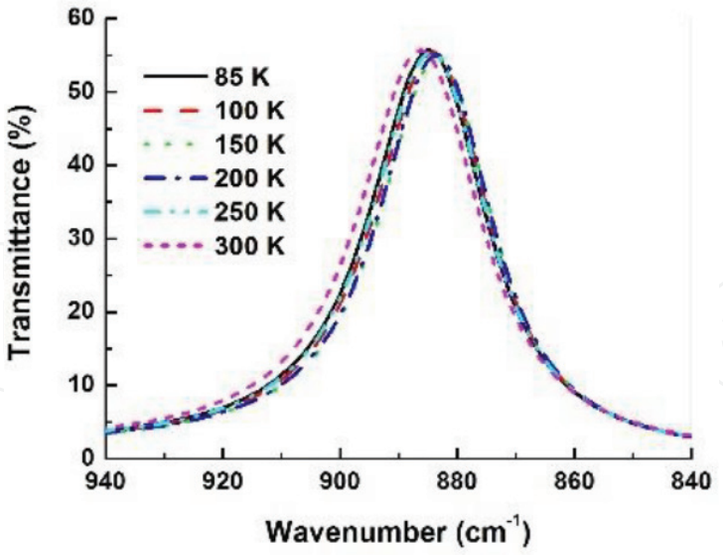

Figure 5. The spectral characteristics of a simple one-cavity Fabry-Perot filter measured in the temperature range of 85–300 K, which was fabricated using $Pb_{0.79}Ge_{0.21}Te$ as high-index evaporation material and ZnSe as low-index layers (ref. [35], reuse permission obtained from OSA).

peak wavelength of 11.30 μm and fabricated using ZnSe as the low-index layer. For its high-index layers, the ingots of $Pb_{1-x}Ge_xTe$ (x = 0.21) were used as the evaporants, from which the layers with corresponding stoichiometry of $(Pb_{0.86}Ge_{0.14})_{0.46}Te_{0.54}$ can be obtained using molybdenum boat evaporation. It can be observed that when ambient temperature changes from 300 to 85 K, a shift of peak wavelength of 0.05935 nm K^{-1} has been achieved for this narrow bandpass interference filter.

3.3. Homogeneity of composition in evaporated layers of $Pb_{1-x}Ge_xTe$

It is commonly believed that the existence of inhomogeneity of composition in layers of $Pb_{1-x}Ge_xTe$ will have a disadvantageous influence on the performance of thin-film interference filters, because the existence of graded Ge concentration profile in $Pb_{1-x}Ge_xTe$ layers will lead into the coexistence of ferroelectric and paraelectric phases at a fixed temperature associated with phase transition as a function of Ge concentration and temperature [40]. Although Partin [41] observed the Ge concentration profile in the layers of $Pb_{1-x}Ge_xTe$ grown on (100) oriented PbTe single crystal by molecular beam epitaxy from PbTe, GeTe, and Te source ovens, to the author's best knowledge, it has still not been clarified whether or not a Ge concentration gradient exists in the layers of $Pb_{1-x}Ge_xTe$ evaporated directly from bulk alloys. Therefore, the investigation on compositional depth profile in evaporated layers of $Pb_{1-x}Ge_xTe$ is of a great significance.

In our investigation, the layers were deposited on silicon wafers using molybdenum boat heating the ingots of $Pb_{1-x}Ge_xTe$, of which compositions were analyzed using energy-dispersive X-ray analysis (EDAX) in a Hitachi S-520 scanning electron microscope. Depth distribution of elements was measured by using a Microlab 301F Scanning Auger Microprobe (SAM) system combined with a discontinuous ion sputtering mode at a base pressure below 8.0×10^{-8} Pa.

http://dx.doi.org/10.5772/intechopen.79272

The results from our investigation are not in agreement with those reported by Partin. In **Figure 6**, a representative compositional depth profile was illustrated for an evaporated layer of $Pb_{1-x}Ge_xTe$, of which the measured elemental concentrations are 42.92 ± 0.55 for Pb, 54.96 ± 0.90 for Te, and 2.12 ± 0.74 for Ge, respectively. It can be observed that the Ge concentration at the surface is lower than that of the stoichiometry, meanwhile, the Pb concentration was distinctly higher. However, the Ge concentration increases from a Ge-deficient state at near surface to the Ge-rich one at near substrate. At same depth, all concentrations of elements remain balanced, that is, the increase of the Ge concentration must be accompanied with a decrease of the Pb concentration. After removal of the upper layers with a thickness of about 300 nm, the layer of $Pb_{1-x}Ge_xTe$ transforms to the Te-deficient characteristic from the Te-rich one. In addition, a stepwise change of elemental concentrations in the depth profile cannot be detected in the layer.

In fact, the mechanism of evaporating from an alloy is much more complicated than that from a single metal because of the different vapor pressures of their individual components. It is much more possible that Ge partial pressure will change with the increasing of deposition time because Ge is more volatile than other components, Pb and Te, in the $Pb_{1-x}Ge_xTe$ alloy. Thereby, Ge concentration in the evaporants will be gradually depleted and the deposition process will result in a compositional gradient in the layers. As a consequence, the results obtained in the compositional depth profiles in evaporated layers of $Pb_{1-x}Ge_xTe$ can be reasonably explained.

Because it is often problematic to maintain a desired alloy in layers and over larger substrate surfaces, therefore, an empirical procedure may be used to determine how to control the composition of the layers by adjusting the composition of the bulk alloy.

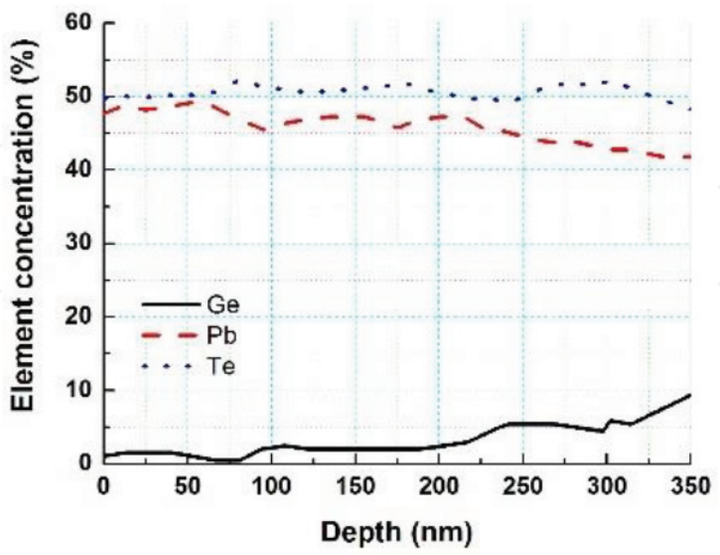

Figure 6. A representative compositional depth profile for an evaporated layer, of which the measured elemental concentrations are 42.92 ± 0.55 for Pb, 54.96 ± 0.90 for Te, and 2.12 ± 0.74 for Ge, respectively (ref. [40], reuse permission obtained from SPIE).

3.4. Compositional dependence of absorption edges in evaporated layers of $Pb_{1-x}Ge_xTe$ and tunable infrared short wavelength cutoff filters

An ideal cutoff filter should have small losses in the transmission region and high attenuation or reflectance in the rejection region over an extended spectral range, which can be carried out depending on interference or absorption [42]. Therefore, a cutoff filter may take a number of different forms, such as interference cutoff filters and thin-film absorption filters.

A thin-film absorption filter usually has very high rejection in the stop region and consists of a layer of material which has an absorption edge at the required wavelength. It is usually short wavelength cutoff in character. A layer of semiconductor that exhibits a very rapid transition from opacity to transparency at the intrinsic absorption edge is a good example to make an excellent thin-film short wavelength cutoff absorption filter. Nevertheless, as far as a layer of a certain semiconductor, such as Ge or PbTe, is concerned, the absorption filter is inflexible in character and the cutoff wavelength cannot be tuned, because of their fundamental optical properties. In order to take advantage of the characteristic of deep rejection of thin-film absorption filters, it will be of great significance to find out a semiconductor material, of which the absorption edge position can be tuned by means of controlling the composition of its layers, to fabricate the absorption filter.

In our investigation, the layers were deposited on silicon wafers using molybdenum boat heating the ingots of $Pb_{1-x}Ge_xTe$, of which compositions were analyzed using energy-dispersive X-ray analysis (EDAX) in a Hitachi S-520 scanning electron microscope. The optical transmission spectra of the layers were measured in the spectral range of 2.5–25 μm using a Perkin Elmer Spectrum GX Fourier-Transform Infrared Spectrometer with a resolution of 8 cm^{-1} at normal incidence. The crystallographic structures of the layers were investigated by X-ray-diffraction (XRD) using Cu K_α radiation on a D/max 2550 V diffractometer with an accuracy of 0.02°. The single-phase nature and polycrystalline of the layers were revealed. The composition dependence of positions of the fundamental absorption edges in the evaporated layers of $Pb_{1-x}Ge_xTe$ was explored. The aim is to elucidate that the tunability of the cutoff wavelength in thin-film absorption filters can be reached if the controllability of the composition of constituent layers can be carried out.

It is revealed that for the evaporated layers of $Pb_{1-x}Ge_xTe$ with an identical Te concentration, the absorption edges will shift toward short wavelength with the increase of Ge concentration x in layers, an example was illustrated in **Figure 7(a)**; furthermore, for those with a similar Ge concentration within a small range of deviation, the edges will also shift toward the short wavelength with Te concentration approach to stoichiometry, an example was illustrated in **Figure 7(b)**.

Our investigation indicates that if the controllability of the composition of evaporated layers of $Pb_{1-x}Ge_xTe$ can be carried out, it will be possible to fabricate an infrared single-layer thin-film absorption filter with the short wavelength cutoff at the required wavelength.

3.5. Compositional congruency, correlation and high-pressure polymorphism in electron-beam evaporated layers of $Pb_{1-x}Ge_xTe$

Currently, evaporation, as a physical vapor deposition process, is still principally used in optical coating industry, because of its simplicity, flexibility and relatively low cost; moreover,

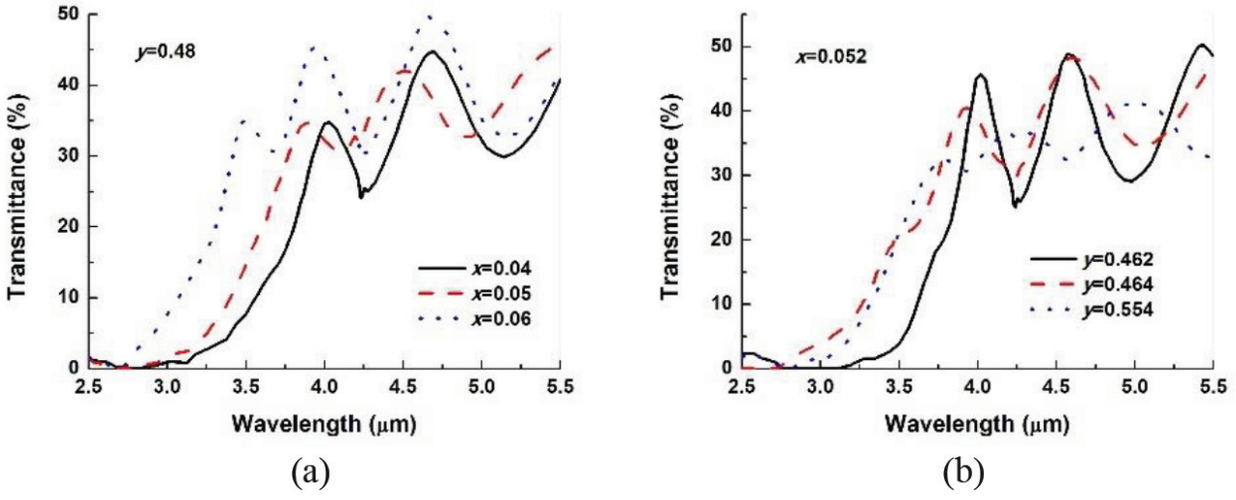

Figure 7. (a) An example to illustrate that the absorption edges will shift toward short wavelength with the increase of Ge concentration x in layers and (b) an example for the edges will also shift toward the short wavelength with Te concentration approach to stoichiometry (ref. [42], reuse permission obtained from SPIE).

the enormous number of existing deposition systems [3]. However, it may be undesirable from a practical viewpoint to evaporate compound semiconductors from a single source because the vapor compositions of compound semiconductors are usually different from their nominal compositions. As a consequence, the stoichiometry of the layers will differ generally from the evaporants [43].

In our investigation, the ingots with different Ge concentrations were chosen and evaporated using the molybdenum boat heating; meanwhile, the ingots with five Ge concentrations, $x = 0.10$, 0.14, 0.17, 0.20, and 0.22, together with PbTe, were evaporated using electron-beam heating. The stoichiometry of the evaporated layers was determined using the energy-dispersive X-ray analysis from a Horiba EX-220 energy dispersive X-ray microanalyzer (model 6853-H) attached to a Hitachi S-4300 cold field emission scanning electron microscope (FE-SEM) without coating the surfaces.

In **Figure 8(a)**, for the layers of $Pb_{1-x}Ge_xTe$ evaporated using electron beam heating, the change of Ge and Te concentration, that is, y and z, with the increasing of Ge concentration in evaporants, x, was illustrated. Similarly, in order to make a clear comparison, for layers evaporated using molybdenum boat heating, the dependence of y and z on x, was also described in **Figure 8(b)**.

It can be observed that Ge concentration y in layers evaporated using electron beam heating is approaching to Ge concentration x of the ingots. A green line that designates an exact linear relation $y = x$ serves as a guideline for the eye in the figure. In comparison with the compositional dependence presented in **Figure 8(b)** for the layers evaporated using molybdenum boat heating, therefore, it can be concluded that electron beam evaporation is a more effective congruent-transfer technique to deposit the layers of $Pb_{1-x}Ge_xTe$ directly from the original $Pb_{1-x}Ge_xTe$ evaporants.

Furthermore, with an increasing of Ge concentration, it can be obviously observed that concentration of tellurium z gradually decreases in the layers evaporated using both electron beam

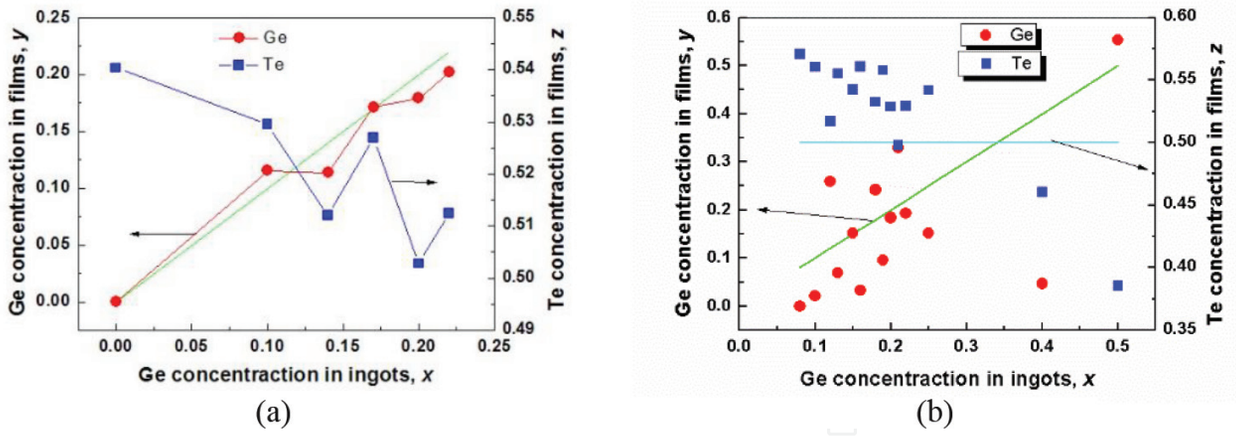

Figure 8. The change of Ge concentration y and Te concentration z in the layers with the increasing Ge concentration in evaporants x, (a) evaporated using electron beam heating, a green line that designates an exact linear relation $y = x$ serves as a guideline for the eye; (b) evaporated using molybdenum boat heating, a green line that designates an exact linear relation $y = x$, and a blue line that represents an exact stoichiometry $z = 50$ for Te concentration in thin films serves as guideline for the eyes, respectively (ref. [43], reuse permission obtained from Elsevier).

and resistance heating. As a consequence, the Te-rich characteristics presented in the layers will shift into the Te-deficient one with the increasing of Ge concentration.

Perhaps, the congruency in the process of evaporation of $Pb_{1-x}Ge_xTe$ using electron beam heating of ingots can be attributed to the "ablation" characteristics of electron beam evaporation and lower thermal conductivity of the PbTe-based alloy. A significant feature of an electron beam evaporator is its ability to concentrate a large amount of power onto a small area of the surface of evaporants, independent of materials being heated. Usually when the evaporants are heated, water cooling is supplied to the crucible to remove the heat which escapes by conduction through the evaporants and liner. In addition, it has been well accepted that PbTe-based alloys constitute a category of materials with excellent thermoelectric figure of merit, zT, because PbTe has a rather lower value of thermal conductivity (2.3 W m^{-1} K^{-1}) [44]. Therefore, when electron beam is focused on the surface of the ingots of $Pb_{1-x}Ge_xTe$, the heat is hardly conducted out and a great temperature gradient is established in the ingots accompanied by the water-cooled crucible. As a consequence, due to the absorption of high energy density by only a small fraction of the ingots irradiated by electron beam, the evaporation behaves like "ablation" with a nonequilibrium nature, at which energy absorbed is much higher than that needed for evaporation, namely, vaporization is independent on the vapor pressures of the constituents.

Furthermore, in our investigation, an assumption can also be proposed to explain the compositional correlation observed in the layers of $Pb_{1-x}Ge_xTe$. It has been well known that the ionic radii of Ge and Pb are 0.73 and 1.2 Å, respectively; therefore, $Pb_{1-x}Ge_xTe$ belongs to a class of alloys in which a substitutional atom has a size significantly smaller than that of the host atom it replaces. In such a "diluted" alloy, the addition of even a very small number of substitutional atoms will lead to a substantial change in their physical properties. For example, although PbTe itself is not ferroelectric, the addition of even 0.05% Ge to PbTe will induce a structural transition [24]. It is obvious that in such a ternary alloy, due to the substitution of Ge ions for Pb ions, two

types of nearest-neighbor bonds, Pb—Te and Ge—Te, must be concerned. Thus, if only the strength of a Ge—Te bond is weaker than that of Pb—Te bond, the amount of Te ions which are incorporated into the system of $Pb_{1-x}Ge_xTe$ will decrease with the increasing of Ge concentration in the layers.

Our assumption can be supported from the experimental data of bond energies reported by Rao and Mohan [45]. It is pointed out that Ge—Te has a bond energy of 1.87 eV, whereas Pb—Te has a bond energy of 1.90 eV; therefore, Ge ions cannot "hold" Te ions as tight as Pb ions do. When the more Ge ions are placed on the Pb site, the more Te ions will "escape." Therefore, the gradual decreasing of Te concentration will make a Te-rich characteristic in layers shift into a Te-deficient one.

In **Figure 9**, the patterns of XRD analysis were demonstrated for the layers evaporated using electron beam heating the ingots with Ge concentration x = 0.10, 0.14, 0.17, 0.20, and 0.22, respectively. It is worthwhile to note that the results for the layers evaporated from ingots with x = 0.22 have some important features. First of all, a new peak can be found, which corresponds to the strongest (111) reflection of rock salt-type structure of GeTe (space-group o_h^5) as referred in JCPDS card number 65-0315. Although the intensity is weak, it can be revealed that

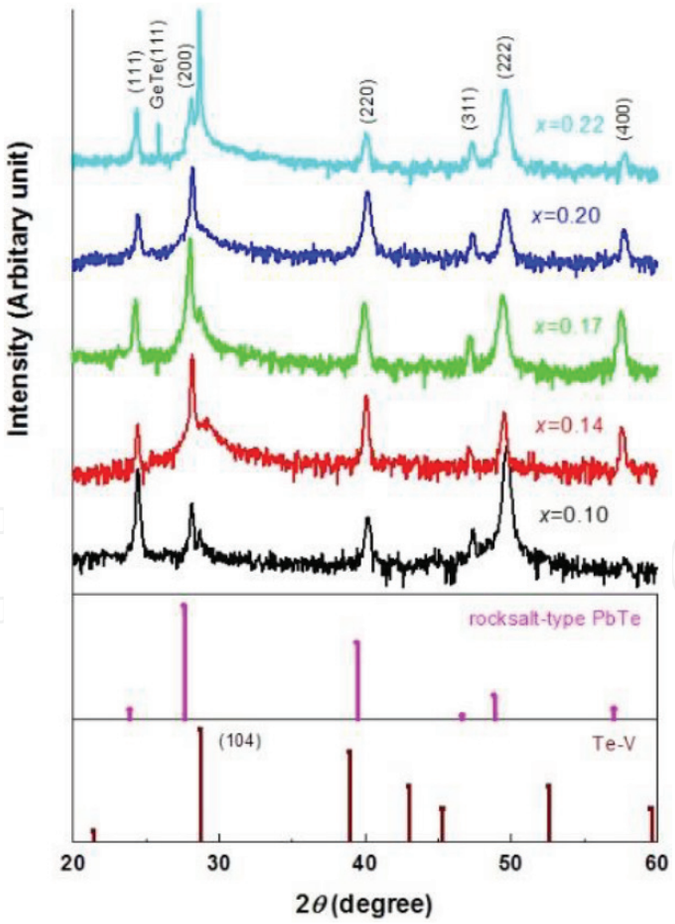

Figure 9. The patterns of XRD analysis for layers evaporated using electron beam heating from ingots with Ge concentration x = 0.10, 0.14, 0.17, 0.20, and 0.22 (ref. [43], reuse permission obtained from Elsevier).

a secondary phase GeTe emerges in the layers. Furthermore, the strongest reflection is different from that in the layers of $Pb_{1-x}Ge_xTe$ with a high temperature paraelectric phase. A strongest peak is expected to occur at $2\theta = 27.58°$, which stands for the (200) plane in PbTe and discloses a highly textured with (001) plane parallel to the silicon substrate. However, the strongest reflection can be attributed to a (111) reflection of substrate silicon (space-group o_h^5) and (104) reflection of a highly symmetric body-centered cubic (bcc) structure Te-V (space-group o_h^9). In order to make a clear elucidation, the position and intensity of reflections given in the JCPDS cards for rock salt-type PbTe and bcc structure Te-V were also added in **Figure 9**, respectively. Therefore, it can be concluded that high-pressure phases for GeTe and Te compounds are also presented in evaporated layers of $Pb_{1-x}Ge_xTe$, which are commonly generated at the higher pressure applying hydrostatic pressure (such as diamond anvil cell) or shock loaded techniques. Perhaps, the transition from the disorder to the order in the system of $Pb_{1-x}Ge_xTe$, which is responsible for ferroelectric phase transition, induces high pressure polymorphism in evaporated layers. Of course, more evidence is furthermore needed.

3.6. The mechanical properties of evaporated layers of $Pb_{1-x}Ge_xTe$

As far as the single-crystal of PbTe is concerned, the microhardness is relatively a constant of ~30 HV for the various carrier concentrations [46, 47]. To the author's best knowledge, no data is reported on hardness of layer of PbTe. However, a layer of PbTe is so soft that it can be scratched easily. As a consequence, an infrared thin-film interference filters consisting of the layers of PbTe is not robust enough to withstand the damage originated from standard wafer dicing processing, such as "from wafer to chips," even if more robust low-index materials, like ZnSe or ZnS, are chosen as an outermost layer.

Therefore, as a solution to the problem in integrating of the standard semiconductor process into the mass-production of infrared thin-film interference filters, a new infrared high-index coating material is needed to deposit the more robust high-index layers to withstand the damages in wafer dicing processing. It is necessary to investigate the mechanical properties of evaporated layers of $Pb_{1-x}Ge_xTe$.

In our investigation, the layers of $Pb_{1-x}Ge_xTe$ were deposited on silicon wafers using electron beam evaporation, of which compositions were analyzed using energy-dispersive X-ray analysis (EDAX) in a Horiba EX-220 energy-dispersive X-ray microanalyzer (model 6853-H) attached to the FE-SEM without coating the surfaces of the layers. Nanoindentation measurements were performed using a Nano Indenter G200 with a three-side pyramidal Berkovich diamond indenter of 50 nm radius under the continuous stiffness measurement (CSM) option. At least 10 indents were performed on each layer with a maximum load of 13 mN, accompanied with a corresponding indentation depth no more than 500 nm. Following the analytic method proposed by Oliver and Pharr [48], the average values and standard deviations of the hardness and Young's modulus of thin films were extracted from the load–displacement results.

It can be revealed that the layers of $Pb_{1-x}Ge_xTe$ have greater values of hardness and Young's modulus compared with those of PbTe. For example, from **Figure 10(a)**, it can be found that

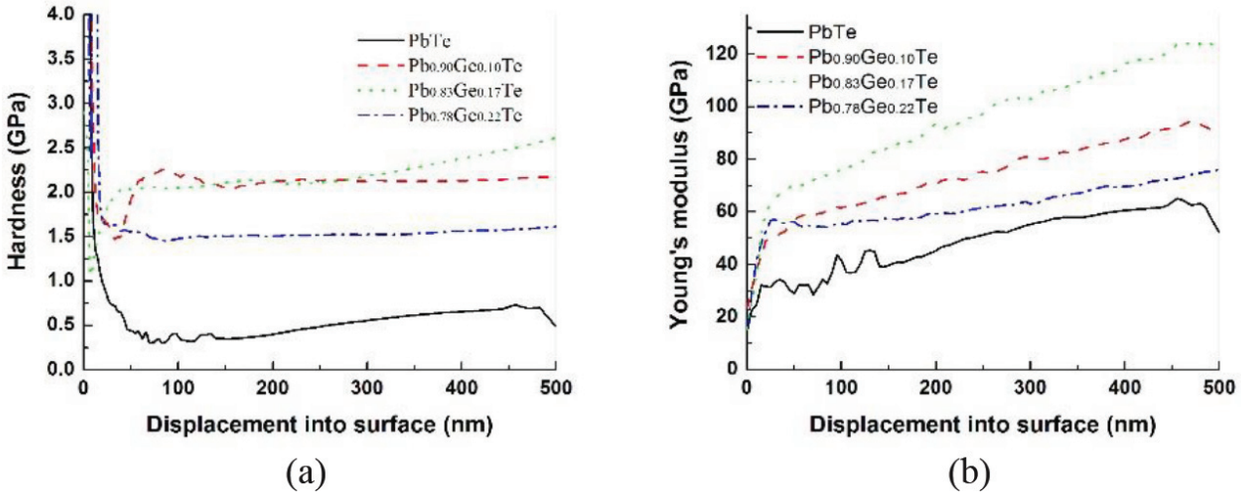

Figure 10. A comparison of the hardness and Young's modulus of the layers evaporated from ingots with three Ge concentrations *x*, 0.10, 0.17, and 0.22, to those of PbTe: (a) the hardness and (b) the Young's modulus (ref. [46], reuse permission obtained from Springer).

the hardness of the layer of $Pb_{0.83}Ge_{0.17}Te$ is three times as great as that of PbTe; meanwhile, Young's modulus is twice greater than that of PbTe, as seen in **Figure 10(b)**. Therefore, a conclusion can be drawn that a mechanically robust infrared high-index layer can be obtained using $Pb_{1-x}Ge_xTe$ as evaporation materials.

These mechanical behaviors of layers of $Pb_{1-x}Ge_xTe$ can be linked to the ferroelectric phase transition. Moreover, the strength loss in the layers can be also explained in light of strong localized elastic-strain fields in concentrated solid solutions.

4. Conclusion

Since Seeley et al. begun the employment of PbTe into the design and manufacture of infrared thin-film interference filters in Infrared Multilayer Laboratory at the University of Reading in 1960s, half of a century has passed. Nowadays, PbTe is still the first choice for the design of infrared thin-film interference filters operating in the long wavelength infrared both at room and cryogenic temperature. In the beginning of this century, aiming at the further improvement of the performance of PbTe, the investigations into $Pb_{1-x}Ge_xTe$ were started up in Shanghai Institute of Technical Physics, Chinese Academy of Sciences. Nowadays, many fruits have been harvested after more than a decade passed.

First of all, it can be concluded that the electron beam evaporation can prove itself a promising powerful tool to make sure the congruent-deposition of the layers of $Pb_{1-x}Ge_xTe$ directly from original $Pb_{1-x}Ge_xTe$ evaporants. Therefore, because the controllability of the composition of evaporated layers of $Pb_{1-x}Ge_xTe$ can be carried out, $Pb_{1-x}Ge_xTe$ will be a prospective infrared high-index material in thin-film interference filters, due to its tunable optical properties corresponding to its intrinsic ferroelectric phase transition, such as temperature coefficient of refractive index and fundamental absorption edge. Furthermore, because the layers of $Pb_{1-x}Ge_xTe$

have superior mechanical properties, such as the hardness and Young's modulus, to those of PbTe, an infrared thin-film interference filters consisting of them will be robust enough to withstand the damage originated from standard wafer dicing processing. As a consequence, the integration of the standard semiconductor process into the mass-production of infrared thin-film interference filters can be also realized.

In addition, one main challenge that needs to be addressed is the toxicity of lead and tellurium. In particular, some issues are concerned regarding the massive use of them in technology due to the toxicity, high costs, and scarcity. In fact, as far as an infrared thin-film interference filter is concerned, the low-index materials, like ZnSe or ZnS, are chosen as an outermost layer so that the layers of PbTe or $Pb_{1-x}Ge_xTe$ are extremely well encapsulated between two adjacent layers of ZnSe or ZnS, followed by careful edge sealing, in order to reduce the hazards of Pb and Te exposure. Furthermore, at the end of the module lifetime, it is important to ensure that all materials be recycled, as already happens for all of the products of infrared thin-film interference filters. However, it would be desirable to find alternatives which retain the unique optical properties of PbTe and $Pb_{1-x}Ge_xTe$. Currently, an investigation is in progress in Shanghai Institute of Technical Physics, Chinese Academy of Sciences to seek an environmentally-friendly, cost-efficient alternative to PbTe-based infrared high-index coating materials.

Acknowledgements

All authors are sincerely grateful to contributions from Prof. Fengshan Zhang and Mr. Ling Zhang (Shanghai Institute of Technical Physics, Chinese Academy of Sciences), Dr. Bin Fan (Optorun Co., Ltd.) and Prof. Jinchun Jiang (East China Normal University). Many thanks to Mrs. Ling Yu (Shanghai Institute of Ceramics, Chinese Academy of Sciences) for the AES analyzes; to Mr. Yuehong Hong and Dr. Guofeng Cheng (Shanghai Institute of Ceramics, Chinese Academy of Sciences) for the XRD analyzes; to Prof. Xianghua Nan (Shanghai Jiao Tong University) and Prof. Xiangming Meng (Technical Institute of Physics and Chemistry, Chinese Academy of Sciences) for the EDAX analyzes; to Dr. Jinlong Li (Ningbo Institute of Industrial Technology, Chinese Academy of Sciences) for his support in the nanoindentation measurements.

Conflict of interest

We declare that we have no conflict of interest.

Author details

Bin Li*, Ping Xie, Suying Zhang and Dingquan Liu

*Address all correspondence to: binli@mail.sitp.ac.cn

Shanghai Institute of Technical Physics, Chinese Academy of Sciences, Shanghai, China

References

[1] Bauer C, Sharma AK, Willer U, Burgmeier J, Braunschweig B, Schade W, Blaser S, Hvozdara L, Müller A, Holl G. Potentials and limits of mid-infrared laser spectroscopy for the detection of explosives. Applied Physics B: Lasers and Optics. 2008;**92**:327-333. DOI: 10.1007/s00340-008-3134-z

[2] Piegari A, Sytchkova AK, Jiri B, Harnisch B, Wuttig A. Thin-film filters for a high resolution miniaturized spectrometer. Proceedings of SPIE. Advances in Optical Thin Films III. 2008;**7101**:710113. DOI: 10.1117/12.797286

[3] Macleod HA. Thin-Film Optical Filters. 4th ed. Boca Raton: CRC Press; 2010

[4] Altaite, From Wikipedia. Available from: https://en.wikipedia.org/wiki/Altaite [Accessed: April 4, 2018]

[5] Singh V, Lin PT, Patel N, Lin HT, Li L, Zou Y, Deng F, Ni CY, Hu JJ, Giammarco J, Soliani AP, Zdyrko B, Luzinov I, Novak S, Novak J, Wachtel P, Danto S, Musgraves JD, Richardson K, Kimerling LC, Agarwal AM. Mid-infrared materials and devices on a Si platform for optical sensing. Science and Technology of Advanced Materials. 2014;**15**:014603. DOI: 10.1088/1468-6996/15/1/014603

[6] Wang JF, Hu JJ, Becla P, Agarwal AM, Kimerling LC. Room-temperature oxygen sensitization in highly textured, nanocrystalline PbTe films: A mechanistic study. Journal of Applied Physics. 2011;**110**:083719. DOI: 10.1063/1.3653832

[7] Böberl M, Fromherz T, Roither J, Pillwein G, Springholz G, Heiss W. Room temperature operation of epitaxial lead-telluride detectors monolithically integrated on midinfrared filters. Applied Physics Letters. 2006;**88**:041105. DOI: 10.1063/1.2167396

[8] LaLonde AD, Pei YZ, Wang H, Snyder GJ. Lead telluride alloy thermoelectrics. Materials Today. 2011;**14**:526-532. DOI: 10.1016/S1369-7021(11)70278-4

[9] Harman TC, Taylor PJ, Walsh MP, LaForge BE. Quantum dot superlattice thermoelectric materials and devices. Science. 2002;**297**:2229-2232. DOI: 10.1126/science.1072886

[10] Heremans JP, Jovovic V, Toberer ES, Saramat A, Kurosaki K, Charoenphakdee A, Yamanaka S, Snyder GJ. Enhancement of thermoelectric efficiency in PbTe by distortion of the electronic density of states. Science. 2008;**321**:554-557. DOI: 10.1126/science.1159725

[11] Seeley JS, Smith SD. High performance blocking filters for the region 1–20 μ. Applied Optics. 1966;**5**:81-86. DOI: 10.1364/AO.5.000081

[12] Evans CS, Hunneman R, Seeley JS. Optical thickness changes in freshly deposited layers of lead telluride. Journal of Physics D: Applied Physics. 1976;**9**:321-328. DOI: 10.1088/0022-3727/9/2/022

[13] Zhang KQ, Hunneman R, Seeley JS, Hawkins GJ. Optical and semiconductor properties of lead telluride coatings. Proceedings of SPIE. Thin Films in Optics. 1989;**1125**:45-52. DOI: 10.1117/12.961354

[14] Evans CS, Hunneman R, Seeley JS, Hawkins GJ, Hunneman R, Seeley JS. Preliminary results from the infrared multilayer filters and materials exposed to the space environment on the NASA LDEF mission. Proceedings of SPIE. Infrared Technology and Applications. 1990;**1320**:407-419. DOI: 10.1117/12.22348

[15] Hawkins GJ, Stolberg-Rohr T. Determination of the embedded thermo-optical expansion coefficients of PbTe and ZnSe thin film infrared multilayers. Optics Express. 2015;**23**: 16348-16355. DOI: 10.1364/OE.23.016348

[16] Stolberg-Rohr T, Hawkins GJ. Spectral design of temperature-invariant narrow bandpass filters for the mid-infrared. Optics Express. 2015;**23**:580-596. DOI: 10.1364/OE.23.000580

[17] Hawkins GJ, Sherwood R, Djotni K, Threadgold T. Cooled optical filters for Q-band infrared astronomy (15–40 μm). Proceedings of SPIE. Advances in Optical and Mechanical Technologies for Telescopes and Instrumentation II. 2016;**9912**:991235. DOI: 10.1117/12.2231669

[18] Walton AK, Moss TS. Determination of refractive index and correction to effective electron mass in PbTe and PbSe. Proceedings of the Physical Society. 1963;**81**:509-513. DOI: 10.1088/0370-1328/81/3/319

[19] Infrared Multilayer Laboratory, Experts in thin film optical coatings. Available from: http://www.reading.ac.uk/infrared/ [Accessed: April 4, 2018]

[20] Sinha NLP, Chaudhuri AK, Bose HN. Structural analysis of lead telluride films and their sensitization. Physica Status Solidi. 1977;**44**:K127-K130. DOI: 10.1002/pssa.2210440253

[21] Yen YH, Zhu LX, Zhang WD, Zhang FS, Wang SY. Study of PbTe optical coatings. Applied Optics. 1984;**23**:3597-3601. DOI: 10.1364/AO.23.003597

[22] Li B, Zhang SY, Zhang FS, Ling Z. Crystal structure, morphology, depth profile of elements and mid-infrared optical constants of 'mild' lead telluride film. Applied Physics A: Materials Science & Processing. 2003;**76**:965-968. DOI: 10.1007/s00339-002-1948-9

[23] Wooley JC, Nikolic P. Some properties of GeTe-PbTe alloys. Journal of the Electrochemical Society. 1965;**112**:82-84. DOI: 10.1149/1.2423473

[24] Hohnke DK, Holloway H, Kaiser S. Phase relations and transformations in the system PbTe-GeTe. Journal of Physics and Chemistry of Solids. 1972;**33**:2053-2062. DOI: 10.1016/S0022-3697(72)80235-X

[25] Antcliffe GA, Bate RT, Buss DD. On the ferroelectric nature of the cubic-rhombohedral phase transition in $Pb_{1-x}Ge_xTe$. Solid State Communications. 1973;**13**:1003-1006. DOI: 10.1016/0038-1098(73)90418-3

[26] Katayama S, Murase K. Role of local displacement of Ge ions on structural instability in $Pb_{1-x}Ge_xTe$. Solid State Communications. 1980;**36**:707-711. DOI: 10.1016/0038-1098(80)90214-8

[27] Suski T. Low-temperature carrier scattering anomalies in ferroelectric $Pb_{1-x}Ge_xTe$. Journal of Physics C: Solid State Physics. 1984;**17**:L689-L696. DOI: 10.1088/0022-3719/17/26/006

[28] Takano S, Kumashiro Y, Tsuji K. Resistivity anomalies in $Pb_{1-x}Ge_xTe$ at low temperatures. Journal of the Physical Society of Japan. 1984;**53**:4309-4314. DOI: 10.1143/JPSJ.53.4309

[29] Bangert E, Bauer G, Fantner EJ, Pascher H. Magneto-optical investigations of phase-transition-induced band-structure changes of $Pb_{1-x}Ge_xTe$. Physical Review B. 1985;**31**: 7958-7978. DOI: 10.1103/PhysRevB.31.7958

[30] Islam QT, Bunker BA. Ferroelectric transition in $Pb_{1-x}Ge_xTe$: Extended X-ray-absorption fine-structure investigation of the Ge and Pb sites. Physical Review Letters. 1987;**59**:2701-2704. DOI: 10.1103/PhysRevLett.59.2701

[31] Cockayne E, Rabe KM. Ab initio study of the ferroelectric transition in cubic Pb_3GeTe_4. Physical Review B. 1997;**56**:7947-7961. DOI: 10.1103/PhysRevB.56.7947

[32] Sariel J, Dahan I, Gelbstein Y. Rhombohedral-cubic phase transition characterization of (Pb, Ge)Te using high-temperature XRD. Powder Diffraction. 2008;**23**:137-140. DOI: 10.1154/1.2912439

[33] Li B, Jiang JC, Zhang SY, Zhang FS. Low-temperature dependence of midinfrared optical constants of lead–germanium–telluride thin film. Journal of Applied Physics. 2002;**91**: 3556-3561. DOI: 10.1063/1.1448866

[34] Li B, Zhang SY, Jiang JC, Fan B, Zhang FS. Improving low-temperature stability of infrared thin-film interference filters utilizing the intrinsic properties of IV-VI narrow gap semiconductors. Optics Express. 2004;**12**:401-404. DOI: 10.1364/OPEX.12.000401

[35] Li B, Zhang SY, Jiang JC, Liu DQ, Zhang FS. Recent progress in improving low-temperature stability of infrared thin-film interference filters. Optics Express. 2005;**13**:6376-6380. DOI: 10.1364/OPEX.13.006376

[36] Li B, Zhang SY, Liu DQ, Zhang FS. New advances in improving low-temperature stability of infrared thin-film interference filters. Proceedings of SPIE. Infrared Components and Their Applications. 2005;**5963**:596328. DOI: 10.1117/12.625375

[37] Heath DF, Hilsenrath E, Janz S. Characterization of a 'hardened' ultrastable UV linear variable filter and recent results on the radiometric stability of narrow band interference filters subjected to temperature/humidity, thermal/vacuum and ionizing radiation environments. Proceedings of SPIE. Optical Remote Sensing of the Atmosphere and Clouds. 1998;**3501**:401-411. DOI: 10.1117/12.317748

[38] Blifford H. Factors affecting the performance of commercial interference filters. Applied Optics. 1966;**5**:105-111. DOI: 10.1364/AO.5.000105

[39] Seeley JS, Hunneman R, Whatley A. Temperature-invariant and other narrow-band IR filters containing PbTe, 4-20 μm. Proceedings of SPIE. Contemporary Infrared Sensors and Instruments. 1980;**246**:83-94. DOI: 10.1117/12.959359

[40] Li B, Zhang SY, Liu DQ, Zhang FS. Homogeneity of composition in evaporated $Pb_{1-x}Ge_xTe$ thin films. Proceedings of SPIE. Detectors and Associated Signal Processing II. 2005;**5964**:596410. DOI: 10.1117/12.625042

[41] Partin DL. Growth of lead germanium telluride thin film structures by molecular beam epitaxy. Journal of Vacuum Science and Technology. 1982;**21**:1-5. DOI: 10.1116/1.571714

[42] Li B, Zhang SY, Xie P, Liu DQ. Compositional dependence of absorption edges in evaporated $Pb_{1-x}Ge_xTe$ thin films as infrared short-wavelength cutoff filters. Proceedings of SPIE. Advanced Optical Manufacturing Technologies. 2009;**7082**:70822L. DOI: 10.1117/12.830991

[43] Li B, Xie P, Zhang SY, Liu DQ. Compositional congruency, correlation and high pressure polymorphism in electron-beam evaporated $Pb_{1-x}Ge_xTe$ thin films. The Journal of Alloys and Compounds. 2014;**589**:109-114. DOI: 10.1016/j.jallcom.2013.11.179

[44] Nolas GS, Goldsmid HJ. Thermal conductivity of semiconductors. In: Tritt TM, editor. Thermal Conductivity: Theory, Properties and Applications. New York: Kluwer Academic; 2004. pp. 105-122

[45] Rao KJ, Mohan R. Chemical bond approach to determining conductivity band gaps in amorphous chalcogenides and pnictides. Solid State Communications. 1981;**39**:1065-1068. DOI: 10.1016/0038-1098(81)90209-X

[46] Li B, Xie P, Zhang SY, Liu DQ. Lead germanium telluride: A mechanically robust infrared high-index layer. Journal of Materials Science. 2011;**46**:4000-4004. DOI: 10.1007/s10853-011-5327-9

[47] Crocker AJ, Wilson M. Microhardness in PbTe and related alloys. Journal of Materials Science. 1978;**13**:833-842. DOI: 10.1007/BF00570520

[48] Oliver WC, Pharr GM. An improved technique for determining hardness and elastic modulus using load and displacement sensing indentation experiments. Journal of Materials Research. 1992;**7**:1564-1583. DOI: 10.1557/JMR.1992.1564